https://doi.org/10.5194/bg-2019-340
Preprint. Discussion started: 23 September 2019

Biogeosciences Discussions
Open Access

A New Characterization of the Upper Waters of the central Gulf of México based on Water Mass Hydrographic and Biogeochemical Characteristics

Authors:

Gabriela Yareli Cervantes-Diaz[1], Jose Martín Hernández-Ayón[1,5], Alberto Zirino[6], Sharon Zinah Herzka[7], Victor Camacho-Ibar[5], Ivonne Montes[4], Joël Sudre[3], Juan Antonio Delgado[1,2]

Author affiliations:

[1]Facultad de Ciencias Marinas, Universidad Autónoma de Baja California, Transpeninsular Tijuana-Ensenada, no. 3917, Fraccionamiento Playitas, CP 22860. Ensenada, Baja California, México.
[2]Instituto Tecnológico de Guaymas/ Tec. Nacional de México, Guaymas, Sonora, México.
[3]LEGOS, CNRS/IRD/UPS/CNES UMR 5566, 18 av. Ed Belin, 31401 Toulouse Cedex 9, France
[4]Insitituto Geofisico del Perú. Lima, Perú.
[5]Instituto de Investigaciones Oceanológicas, Universidad Autónoma de Baja California, Transpeninsular Tijuana-Ensenada, no. 3917, Fraccionamiento Playitas, CP 22860. Ensenada, Baja California, México.
[6]Scripps Institution of Oceanography, University of California, San Diego, 9500 Gilman Drive, La Jolla, California 92093, USA.
[7]Departamento de Oceanografía Biológica, Centro de Investigación Científica y de Educación Superior de Ensenada (CICESE), Baja California, Carretera Ensenada-Tijuana No. 3918, Zona Playitas, 22860 Ensenada, Baja California, México.

*Corresponding author
Instituto de Investigaciones Oceanológicas
Universidad Autonoma de Baja California
jmartin@uabc.edu.mx;

Key Points:

Gulf of Mexico, Water masses, oxygen dissolved, biogeochemistry.

https://doi.org/10.5194/bg-2019-340
Preprint. Discussion started: 23 September 2019

Biogeosciences
Discussions

Abstract.

In the Gulf of Mexico (GoM) at least three near-surface water masses are affected by mesoscale processes that modulate the biogeochemical cycles. Prior studies have presented different classifications of water masses where the greater emphasis was on deep waters and not on the surface waters ($\sigma_\theta < 26$ kg·m^{-3}), as in this work. Here presents a new classification of water masses in the GoM, based on thermohaline properties and dissolved oxygen (DO) concentration using data from a total of five summer and winter cruises carried out primarily in the central GoM. The reclassification includes an adjustment to the spatial range of Caribbean Surface Water (CSW), which is detected only during the summer. This water mass extends from the surface to H 90 m and features warm waters (27-32 ºC), high salinities (up to ~36.8), non-detectable nitrate concentration, and negative values of the apparent oxygen utilization (AOU) of H -27 µmol·kg^{-1}. Below the CSW, the deeper Gulf Common Water (GCW) was also redefined and characterized by a subsurface DO maximum, with values H 50 µmol·kg^{-1} higher than that found in surface waters. In winter, a replacement of the CSW by the GCW affected the biogeochemical composition of surface water as observed from an increase in nitrate concentrations, positives values of AOU (H 90 µmol·kg^{-1}) and a decrease in surface temperatures (< 27 ºC). This is because during winter, the Tropical Atlantic Central Water (TACW) that lies below the GCW is closer to the surface and contributes nutrients and low DO via strong vertical mixing induced by the windy "Nortes" season. CARS2009 analysis supports the formation of the subsurface maximum of DO during the summer and disappears in winter. In this work also named surface water that is characterized by a low salt content (H 33.1) from 0 to 20 m as Freshwater Influenced Surface Water (FISW).

https://doi.org/10.5194/bg-2019-340
Preprint. Discussion started: 23 September 2019

Biogeosciences Discussions
Open Access

1. Introduction.

Circulation in the central Gulf of Mexico's (GoM) is dominated by the Loop Current (LC) and its associated eddies. Anticyclonic Loop Current Eddies (LCE) H 200 - 300 km in diameter separate from the LC every 4 to 18 months (Sturges and Leben, 2000; Hall and Leben, 2016). Another feature associated with the LC is the separation of relatively smaller cyclonic and anticyclonic eddies throughout the basin, which interact in an apparently turbulent manner (Schmitz, 2005; Hamilton, 2007a). These eddies extend vertically from a few hundred to about a thousand meters and appreciably influence the surface dynamics by modifying the circulation of the GoM (Morey *et al*., 2003a). The position of the LC within the gulf is variable, and the level of intrusion into the northeastern GoM varies temporally and spatially (Bunge *et al*., 2002; Delgado J. A. *et al*., 2019).

Near the surface, the spatio-temporal variability in temperature, salinity and dissolved oxygen (DO) reflect the LC, LCE and other eddy dynamics, freshwater inputs from river discharge, and seasonal processes such as heat fluxes, evaporation and wind stress that influence the depth of the mixed layer (Morey *et al*., 2003b; Müller-Karger *et al*., 2015; Portela *et al*., 2018; Damien *et al*., 2018). A major source of variability in the northern GoM is the Mississippi River flow, which has been shown to influence areas hundreds of kilometers from its discharge zone (Morey *et al*., 2003a) over the first 50 m of the water column (Jochens & DiMarco, 2008; Portela *et al*., 2018). Together, the aforementioned mechanisms influence water mass characteristics in approximately the first 250 m (or more) of the water column. For example, upon entering the GoM, the Caribbean Surface Water (CSW) affects salinity, temperature, and density with values of 34.5 to 36.6; T ≥ 25 ºC, and

https://doi.org/10.5194/bg-2019-340
Preprint. Discussion started: 23 September 2019

$\sigma_\theta \leq 24.5$ kg·m^{-3} (Carrillo *et al.*, 2016). Below the CSW, North Atlantic Subtropical Underwater (NASUW, hereinafter referred to as SUW) can be identified by a salinity between 36.5 to 36.9 at H 100 to 150 m (Herrig, 2010; Hamilton *et al.*, 2018). The Gulf Common Water (GCW) is distinguished by the relatively homogeneous vertical distribution of its thermohaline properties, with salinity ranging from 36.3 to 36.49 (Elliott, 1982; Merrell and Morrison, 1981). Underneath the SUW and GCW, Tropical Atlantic Central Water (TACW) is found between 300 and 600 m, and is characterized by a DO minimum of 2.3 ml·L^{-1}, T from 7.9 to 20 °C, S from 34.9 to 36.6, and σ_θ from 26.25 to 27.2 kg·m^{-3} (Vidal *et al.*, 1994; Gallegos, 1996; Carrillo *et al.*, 2016; Portela *et al.*, 2018). The main sources of variability in the physical and chemical properties of the surface to approx. 250 m (above 26 kg·m^{-3}) can be related to changes in the relative proportions of water masses.

There have been limited surveys of the hydrographic characteristics of the central GoM and Yucatan Channel within Mexico's Exclusive Economic Zone (including the Campeche Basin (CB)) based on *in situ* data, and of those, several have been limited to relatively small regions: For example, Morrison *et al.* (1983) studied the distribution of physical-chemical properties of the water masses (GCW, TACW, Antarctic Intermediate Water (AAIW) and the mixture of Caribbean Intermediate Water (CIW) and North Atlantic Deep Water (NADW) and the NADW) in the northwestern GoM during winter. Similarly, Vidal *et al.* (1994) also investigated the spatial distribution of thermohaline properties and DO of the GCW, SUW, TACW, AAIW, as well as the mixture between CIW and NADW, and NADW in the western region of the GoM during winter and spring. Among these efforts, Rivas *et al.* (2005) studied the area of the Yucatan Channel, they found five different water masses (SUW, 18º SSW,

https://doi.org/10.5194/bg-2019-340
Preprint. Discussion started: 23 September 2019

TACW, AAIW y NADW). Finally, Hamilton *et al*. (2018) performed an analysis with high-resolution data from the deeper waters (SUW, AAIW y NADW) of the western and eastern in the GoM, with results that were consistent with the findings of the previous authors. Obviously, different water masses may be present depending on the region of the GoM that is being studied.

In particular, the above authors focused on the role of the dominant LCE's on the hydrographic characteristics of the central and western GoM (Fig. 1a). However, their proposed classification did not include near-surface waters; for example, lower salinities (likely due to river inputs) were not included. Excluding water masses with lower salinities in the classification scheme limits the inferences that can be made regarding source waters. This points to the necessity of generating a more detailed classification system in the surface layers above the 26 $kg \cdot m^{-3}$ isopycnals, which includes the full range of thermohaline properties of water masses. When DO concentrations are added to the Θ-S_A diagram as a third axis, it can be observed that DO shows a high variability (> 200 $\mu mol \cdot kg^{-1}$) upwards of the 26 $kg \cdot m^{-3}$ isopycnal (Fig. 1b). This change in DO is a result of biogeochemical processes via, photosynthesis, respiration, and exchange with the atmosphere, which also lead to changes in dissolved inorganic carbon (DIC) and nutrients.

From a biogeochemical perspective, the surface waters of the deep GoM are considered oligotrophic as they are relatively isolated from the more eutrophic waters of the coast and continental shelves (Heileman and Rabalais, 2009; Damien *et al*., 2018; but see Martínez-López y Zavala-Hidalgo, 2009). Near the surface, and far from the coast, low rates of primary production (low than 0.15 g C m^{-2} d^{-1}; Biggs y Ressler, 2001) have been reported; however, productivity in subsurface waters maybe two to three times higher (El-Sayed, 1972; Biggs and Ressler, 2001). Dynamic features such as mesoscale processes, river inputs, the extent of the seasonal LC incursion, and wind stress can greatly alter the distribution of chemical properties in the GoM (Linacre *et al*., 2015; Damien *et al*., 2018). Overall, the effect that water masses have on the seasonal extension of the mixed layer is not well understood, though its deepening and shallowing play an important role in the rates of primary production (Damien *et al*., 2018).

In this work propose a classification for water masses lighter than 26 $kg\cdot m^{-3}$ that more precisely defines the ranges of thermohaline circulation and DO of the CSW and GCW, thereby providing a better basis for understanding the processes associated with water mass formation, distribution, and biogeochemistry in surface waters of the central and western regions of the GoM. Our purpose is to provide a better tool for studying the drivers that modulate water mass distribution and its formation in surface waters, as well as the links between water masses and their biogeochemical properties. The reclassification includes an adjustment of the thermohaline range of CSW and the GCW. In this work also propose the formal recognition of Freshwater Influenced Surface Water (FISW) that is characterized by riverine influence. Finally, examine the role of CSW in the biogeochemistry of the GoM by comparing the seasonal variations in T_θ and S in our *in situ* water to the climatological database CARS 2009.

2. Data and Methods

https://doi.org/10.5194/bg-2019-340
Preprint. Discussion started: 23 September 2019

2. 1. Data collection

Five oceanographic cruises covering the central region of Mexico's Exclusive Economic Zone were carried out in November 2010, July 2011, February-March 2013, August-September 2015, and July 2016 (XIXIMI-01 through XIXIMI-05, respectively) on board the *R/V Justo Sierra* (Fig. 1c). During these campaigns, a minimum of 30 and maximum of 51 stations per cruise were occupied, and a total of 235 hydrographic casts were performed to characterize the vertical distribution of potential temperature (T_θ), salinity (S), potential density (σ_θ), and DO. An SBE 911plus CTD was used; the instrument and sensors were serviced and calibrated regularly.

In addition to CTD casts, water samples were collected for measurements of Dissolved Inorganic Carbon (DIC), nutrients, and DO analyses in 10 or 20 L Niskin bottles at 12 set depths between the surface and bottom. The protocols and best practices established by Dickson *et al.* (2007) were followed for DIC sample collection. For the collection of nutrient samples, 50 ml of seawater were filtered through Whatman GF/F filters previously calcinated at 450 °C for 2 hours, transferred to centrifuge tubes and frozen. Each sample was transported frozen to the laboratory for later analysis. During each cruise, seawater was also routinely sampled for DO (evaluated by the Winkler method) measurements and to calibrate the CTD data. Additionally, the apparent oxygen utilization (AOU) was calculated from DO, T, and S using TEOS-2010 equations. AOU is defined as the deviation of the measured dissolved oxygen from a DO concentration in equilibrium with the atmosphere (Benson and Krause, 1984). When calculating the AOU the DO is corrected for temperature. This allowed us to determine if DO concentrations were in equilibrium with oxygen in the atmosphere.

https://doi.org/10.5194/bg-2019-340
Preprint. Discussion started: 23 September 2019

2. 2. Water masses

2. 2. 1. Identification of water masses

An analysis of T_θ-S diagrams was carried out for the five cruises; T_θ and S were converted to conservative temperature (Θ) and absolute salinity (S_A) as described by McDougall and Barker (2011). For water mass identification, in this work first used the limits described by Vidal *et al*. (1994), Morrison *et al*. (1983) and Nowlin *et al*. (2001) and the recent classification proposed by Portela *et al*. (2018), as shown in figure 1a.

2. 2. 2. Seasonal variation

Two of the five cruises took place during the late fall and winter (2010 and 2013), and three during summer (2011, 2015, and 2016). Since sampling in winter and summer covered approximately the same region of the GoM (Fig. 1c and 3), in this work could perform a separate seasonal analysis of hydrographic and geochemical characteristics for densities lower than 26 $kg \cdot m^{-3}$ in the Θ-S_A diagrams using the Portela *et al*. (2018) classifications (Fig. 2). DO was incorporated into the diagrams to evaluate the role of seasonality on its vertical distribution in relation to water masses. It was noted that the depth of the 26 $kg \cdot m^{-3}$ isopycnal varied by more than 100 m regardless on the time of year (Fig. 3 and Supplementary Fig. 2).

2. 2. 3. T_θ-S patterns above 26 $kg \cdot m^{-3}$

Four patterns were visually identified in the T_θ-S diagrams by focusing on the most distinctive characteristics for densities less than 26 $kg \cdot m^{-3}$ (Fig. 4). The four distinct T_θ-S

https://doi.org/10.5194/bg-2019-340
Preprint. Discussion started: 23 September 2019

patterns (indicated by parallelograms) shown in Table 1 and figure 4 had the following characteristics:

- The blue T_θ-S pattern was characterized by a subsurface salinity maximum and lower concentrations of DO associated with the Subtropical Underwater (SUW) (Fig. 2b and 4).
- The pink T_θ-S pattern was characterized by shallow fresh waters (low than 36; see Table 1) that are likely associated with river inputs and their offshore transport. In this study, this water mass is referred to as Freshwater Influenced Surface Water (FISW) (Fig. 2b and 4).
- The green T_θ-S pattern was observed during summer cruises and was characterized by a wide range of temperatures (23.7 to 27.5ºC; see Table 1) and salinity, and a subsurface DO maximum (H 232 µmol·kg^{-1}) at a density of approximately 24.5 kg·m^{-3}. This pattern is heavily influenced by the CSW.
- The red T_θ-S pattern was observed during winter and had a narrow salinity range (36.4 to 36.6; see Table 1), indicating the limited influence of the CSW coupled with seasonally lower temperatures (22.9 to 23.2 ºC; see Table 1). This so so-called Gulf Common Water (GCW) is closer to the surface during winter.

Finally, in this work carried out a reclassification of the range limits for the water masses lighter than 26 kg·m^{-3}. This reclassification was done using a Matlab program that separated and binned the data based on the four T_θ-S patterns previously described (Table 1): these were then independently plotted to fit individual T_θ-S patterns ranges of the existing

https://doi.org/10.5194/bg-2019-340
Preprint. Discussion started: 23 September 2019

Biogeosciences Discussions
Open Access

classification established by Vidal *et al*. (1994), Morrison *et al*. (1983) and Nowlin *et al*. (2001). A final readjustment was done based using T_θ-S patterns analysis of the existing thermohaline ranges (σ_θ, T_θ, S; Table 1) and the DO concentration of the water masses that were observed in the T_θ-S diagrams. An extended description of the code with the criteria for classification is provided in Appendix A.

2. 2. 4 Analysis of the vertical variability of σ_θ, T_θ and DO in surface waters

Sections of the vertical distribution of σ_θ, T_θ and DO were made for each cruise (2010, 2011, 2013, 2015 and 2016, Fig. 5a-j and 6) to examine differences in the density, temperature and DO to arising from different oceanographic conditions (Fig. 5 and 6).

2. 4. Analysis of chemical variables

To determine the concentration of DIC, coulometric methods were used following the methodology described by Johnson *et al.* (1987). Reference materials were provided by the laboratory of Dr. A. Dickson of Scripps Institution of Oceanography. The accuracy obtained with respect to the reference material was ± 2 $\mu mol \cdot kg^{-1}$ with a precision of ± 1.5 $\mu mol \cdot kg^{-1}$. To quantify the concentrations of combined nitrite and nitrate (NO_2^- + NO_3^-, hereafter, nitrate) present in the samples from the winter 2010 and 2013 cruises, a Skalar SAN Plus autoanalyzer was used. The reference material MOOS-2 was obtained from the National Resource Council Canada. The analytical precision was better than 5% for nitrite and nitrate combined. For the quantification of the summer 2015 cruise, samples were analyzed with an AA3-HR SEAL nutrient analyzer according to the GO-SHIP Repeat Hydrography Manual (Hydes *et al*., 2010) using seawater lots CC and CD from Kanso Co. Ltd. (KANSO Technos,

https://doi.org/10.5194/bg-2019-340
Preprint. Discussion started: 23 September 2019

Japan) as reference materials (see description in Aoyama and Hydes, 2010). Precision is expressed as a coefficient of variation (CV) and was 0.2% for nitrate.

In order to explore possible relationships between water masses and their nitrate and DIC content, T_θ-S vs. nitrate for late fall-winter of 2010 and 2013, and summer of 2015, (respectively) were plotted and T_θ-S vs. DIC diagrams for late fall-winter and summer 2011, 2015 and 2016 (respectively) were also plotted. This allowed for a seasonal comparison.

2. 5. Absolute Dynamic Topography (ADT) maps

Absolute Dynamic Topography (ADT) maps were generated to infer the seasonal influence of the CSW during the different cruises as Delgado *et al.* (2019) suggest. The images are products of the AVISO + database (Archiving, Validation, and Interpretation of Satellite Oceanographic data) available on the website https://www.aviso.altimetry.fr/en/data. The ADT maps only considered the time in which sampling was carried out for each cruise. In this work, present the surface dynamics based on these ADT maps, particularly from our winter (Feb-Mar) 2013 and summer (Aug-Sep) 2015 cruises (Fig. 10b and 10e).

2. 6. Climatological data analysis

An analysis of the temperature and salinity data from the climatological database CARS 2009 (CSIRO Atlas of Regional Seas; http://www.marine.csiro.au/~dunn/cars2009) was performed to contrast climatological averages between *in situ* data from winter (February)

https://doi.org/10.5194/bg-2019-340
Preprint. Discussion started: 23 September 2019

and summer (July). Diagrams and vertical sections reflecting 50 years of monthly July and February T_θ and S data were plotted to identify the seasonal presence or absence of CSW.

Finally, in this work developed the new reclassification of the water masses based on the characteristic of the thermohaline and biogeochemical variables at densities lower than 26 kg·m-3 for each identified water mass.

2. Results

Potential temperature and salinity showed spatial and temporal variability at densities < 26 kg·m-3 during the five sampling campaigns included in this study (Fig. 1b). The four patterns that in this work considered relevant for the designation of new thermohaline ranges for water masses above the isopycnal of 26 kg·m-3, namely CSW, SUW, GCW, and the FISW, are described in the following section.

3.1. Changes in T_θ and σ_θ in presence or absence of CSW

Vertical sections of seasonal changes in potential density and potential temperature occurring in the first H 250 m (above 26 kg·m-3) of the study area are shown in figure 5. In general, the relatively low temperatures (T H24 ºC with ΔT < 5 ºC over densities < 26 kg·m-3; Fig. 5a, and 5b) indicate the absence of CSW in late autumn and winter and show a more mixed column in the first 100 m. Additionally, the density was, on average H 24.5 kg·m-3 (with Δ σ_θ < 1 kg m-3; Fig. 5f and 5g). These characteristics are associated with the near-surface presence of GCW. During the summer, evidence of CSW with a temperature of H 31ºC was

https://doi.org/10.5194/bg-2019-340
Preprint. Discussion started: 23 September 2019

observed with ΔT ± 6 ºC (Fig. 5h, 5i, and 5j). On the other hand, density fluctuated from σ_0 = 22 to 24 kg·m-3 (Fig. 5c, 5d, and 5e).

It is noticeable that during the winter of 2013, when CSW was absent, the 24 kg·m-3 isopycnal and the 27 ºC isotherm were not observed (Fig. 5b, and 5g). In contrast, water with these characteristics was present during the summer when CSW entered the GoM through the LC (Fig. 5c, 5d, 5e, 5h, 5i, and 5j). Therefore, the summer characteristics of density and temperature represent the water of Caribbean origin.

3. 2. Subsurface maximum DO and its association with GCW

In addition to the low density/high temperature waters typical of the CSW, in this work also noted the presence of a summer DO subsurface maximum. Figure 6 displays transects of vertical sections of DO for the five cruises carried out during summer 2011, 2015, and 2016 a DO subsurface maximum of H 210 to 232 µmol·kg-1 is shown to exist (Fig. 6c, 6d, 6e, 7b, and 7c). This pattern was observed consistently in the three summer cruises. The DO maximum was located between the isopycnals of 24 kg·m-3 and 25 kg·m-3 and can be considered a boundary between CSW and GCW. In contrast, with the absence of CSW during late fall (November 2010), the DO subsurface maximum was no longer clearly observable. During winter (February/March 2013), vertical mixing homogenized the DO in the first 200 m to concentrations of 200 to 220 µmol·kg-1 (Fig. 6b).

In this work found that during summer, AOU tends towards negative values (from 2 to -26.5 µmol·kg-1; see Supplementary Fig. 1c-e), above atmospheric equilibrium and supersaturated in waters above densities of H 24 kg·m-3. In contrast, in late autumn and winter, AOU values

https://doi.org/10.5194/bg-2019-340
Preprint. Discussion started: 23 September 2019

Biogeosciences Discussions

in the GCW were positive at the same depths and ranged from 9 to 90 $\mu mol\cdot kg^{-1}$ due to the vertical transport of subsurface water (Supplementary Fig. 1a-b). This suggests that DO and AOU profiles can be used as criteria with which to separate the CSW from the GCW.

3. 3. Description of water masses identification using the new classification. To readjust the thermohaline ranges corresponding to CSW and GCW, oxygen was used as a tracer to separate these two water masses. It is important to note that the thermohaline ranges associated with the SUW were not modified because this water mass is only detected inside the LC. The thermohaline and chemical characteristics of each water mass are described in the following sections.

3. 3. 1. Subsurface Underwater (SUW).

Figure 7 shows the T_θ and S data above the isopycnal of 26 $kg\cdot m^{-3}$ as well as the new limits of salinity and temperature of surface waters (see Table 2). Figure 7a, shows typical oceanographic characteristics of water from the Caribbean, including the horseshoe structure present in T_θ-S diagrams that describe the SUW (Fig. 2 and 4). The principal thermohaline characteristic of the SUW is the presence of a salinity maximum (H 36.9) paired with a relative oxygen minimum (H 137 $\mu mol\cdot kg^{-1}$) located between 150 and 250 m (Fig. 7a). In this work found that SUW typically occurs in summer between 100 to 250 m and transports low oxygen water into the GoM (Table 2).

3. 3. 2. Caribbean Surface Water (CSW)

CSW was only detected during the summers of 2011, 2015 and 2016. DO concentrations varied between 180 to 190 $\mu mol\cdot kg^{-1}$ within the top 30 m of the water column. Surface water

https://doi.org/10.5194/bg-2019-340
Preprint. Discussion started: 23 September 2019

above the 24 kg·m-3 isopycnal that includes the full range of thermohaline properties needs to be better defined. The T and S ranges in this work propose for this water mass are: temperatures between 27 and 32 ºC, salinities between 36 and 36.8, and a DO concentration range of 180 to 220 µmol·kg-1 (Table 2). The presence of CSW can be observed from relatively high salinities (up to H 36.8) accompanied by relatively high surface temperatures of approx. 30 ºC (Fig. 7a, 7b, and 7d).

3. 3. 3. Gulf Common Water (GCW)

The surface water between the 24 and 26 kg·m-3 isopycnals also needs to be defined by including the subsurface DO maximum as the upper limit of GCW. In this work propose new range limits for GCW to be temperatures between 20 to 27 ºC, salinities between 36.3 to 36.6 and DO between 112 to 232 µmol·kg-1 (Fig. 7c, Table 2). Brunt-Väisälä frequency analysis confirms the late fall data from 2010 and winters 2013 indicated vertical mixing in the first 200 m of the water column induced by season "Nortes" (not show figure).

3. 3. 4. Freshwater Influenced Surface Water (FISW)

The presence of the FISW was observed in summer. FISW was detected in the interior region of the CB and was distributed along the 25 ºN transects during 2010, 2011, 2015, and 2016 campaigns (Fig. 7d). This coincided with periods of high precipitation prior to and during the campaigns (https://smn.conagua.gob.mx/es/climatologia/temperaturas-y-lluvias/resumenes-mensuales-de-temperaturas-y-lluvias). Based on the aforementioned thermohaline characteristics and the distribution of this water mass, the following limits were established: temperature between 24 to 30 ºC, salinity between 33 and 36, and DO concentrations between 180 and 220 µmol·kg-1 (Fig. 7d; Table 2).

https://doi.org/10.5194/bg-2019-340
Preprint. Discussion started: 23 September 2019

The input of freshwater resulted in a lowering of surface salinity in the first 20 m below approx. 36 (Fig. 7d). The temperature range was from 24 ºC in late fall of 2010 to 30 ºC during summer (2011, 2015, and 2016).

3. 4. Water mass variability linked to DIC and nitrate concentrations

In general, SUW nitrate concentrations near its T_θ-S upper limit where 0.06 µM at σ_θ H 24.5 kg·m^{-3}) increasing to H 7.1 µM a near its T_θ-S bottom limit, as defined. DIC concentrations were approx. 2098 µmol·kg^{-1} and increased to H 2150 µmol·kg^{-1} at H 250 m (Table 2). The maximum nitrate concentration (H 7 µM) detected in the first 250 m was in the center core of the SUW at σ_θ H 25.4 kg·m^{-3} (Fig. 8a and 8c), while the DIC maximum of H 2152 µmol·kg^{-1} at σ_θ H 25.8 kg·m^{-3} coincided with DO concentrations of H 146 µmol·kg^{-1} (Fig. 7a, and 8d).

As mentioned, the CSW was only detected during the summer oceanographic campaign. This water mass was characterized by low concentrations of nitrate from 0 to 0.48 µM in the first 90 m of the water column (Fig. 8c and 9f; Table 2). Similarly, DIC in this water mass was lower than 2090 µmol·kg^{-1} (Fig. 8d; Table 2).

The GCW contained relatively high concentrations of nitrate during late fall and winter, approx. 2 µM near 75 m. The highest concentrations of nitrate above 200 m, H 8.4 µM was detected during this season, and it was observed within the lower limit of the GCW and the upper limit of the TACW (Fig. 8a; Table 2). In summer, the highest nitrate concentrations of H 1.5 µM were found near 100 m, reaching values of approx. 9.4 µM near the lower limit of

https://doi.org/10.5194/bg-2019-340
Preprint. Discussion started: 23 September 2019

the GCW at H 210 m (Fig. 8c; Table 2). In the GCW, the vertical distribution of DIC mimicked the nitrate profiles. During late fall and winter, DIC concentrations higher than 2080 $\mu mol \cdot kg^{-1}$ were found below 50 m and reached maximum values of 2172 $\mu mol \cdot kg^{-1}$ near the bottom depth of this water mass (Fig. 8b; Table 2).

During summer at 50 m (σ_θ = 24.6 kg m^{-3}), DIC values slightly lower than 2075 $\mu mol \cdot kg^{-1}$ were observed to increase with depth to H 2169 $\mu mol \cdot kg^{-1}$ at H 210 m (Fig. 8d). The deepening of the nutricline and carbocline observed during summer was associated with the transport of oligotrophic waters by CSW into the GoM, with low values of nitrate < 1 µM near the surface (Fig. 8c and 8d; Table 2).

Finally, the chemical composition of FISW depended to a large extent on the seasonality of precipitation, fluvial inputs, and mesoscale dynamics. Stations of low salinity and low nitrate concentrations ranging from 0.02 to 1.27 µM, and DIC ranging from 2005 to 2062 $\mu mol \cdot kg^{-1}$ in the first 50 m of the water column were sampled in winter (Fig. 8a, and 8b; Table 2). In contrast, during summer the concentrations of nitrate and DIC were slightly lower and ranged between 0.08 to 0.34 µM, and 1968 to 2053 $\mu mol \cdot kg^{-1}$, respectively (Fig. 8c, and 8d; Table 2).

4. Discussion.

A recent detailed analysis in the central and western GoM by Portela *et al*. (2018) of water masses from glider data, 14 cruises and Argo floats within the GoM, indicated the presence

https://doi.org/10.5194/bg-2019-340
Preprint. Discussion started: 23 September 2019

of seven water masses. While this is an improvement, there are still some problems in the classification and understanding of waters upwards of the 26 kg·m-3. In this work maintain that it is necessary to have a better understanding of how the GoM's water masses are formed to attain a classification that gives insight into 1) the dynamics of the water masses in the gulf, and 2) the physical mechanisms affecting biogeochemical processes, and 3) the resulting effects within biological processes. Upwards of the 26 kg·m-3 isopycnal, biogeochemical variables, such as oxygen, nitrate, and DIC concentrations exhibit large changes in concentration (≈ 200 μmol·kg-3, 0 and 9 μM, and 160 μmol·kg-3, respectively) that reflect the dynamic and variable characteristics of surface waters. These variations are caused by mixing and advection, processes that are important to be identified and understood. For this reason, it was important to reclassify the shallower water masses of the GoM by including DO as a key tracer.

4. 1. Reclassification of CSW and CGW using T, S and dissolved oxygen

In this work found a noticeable presence of CSW associated with the incursion of the LC during spring-summer as described by Delgado *et al*. (2019); this water mass was absent in late autumn and winter. Recently, the spring-summer incursion of the LC that transports CSW into the GoM has been confirmed, with a maximum presence in summer and a minimum in winter (Delgado *et al*., 2019). In this work emphasize that the extended "pulsing" by the LC and the Yucatán Current into the GoM explains the presence of CSW. In this work attribute this absence of the CSW to the weakening of the LC.

In this work agree that the CSW increases its salt content above the 24 kg·m-3 isopycnal from about 36 at its entry into the GoM in the Yucatan Channel to about 36.8 due to LCE's and

https://doi.org/10.5194/bg-2019-340
Preprint. Discussion started: 23 September 2019

coastal upwelling (Wüst, 1964; Hernández-Guerra and Joyce, 2000; Carrillo *et al.*, 2016). Also, evaporation likely contributes to the increase in salinity, caused by an increase in surface temperature during the summer when CSW is found within the GoM (Fig. 7a, and 7b). Previous studies have reported that the increasing stratification during the summer (mixed layer depth < 40 m) isolates the surface layer of the water column, which results in an increase in salinity due to intense evaporation (Zavala-Hidalgo *et al.*, 2014).

Recently, Portela *et al.* (2018) redefined the T-S limits of the CSW within the GoM, renaming it a remnant of the Caribbean Surface Water (CSWr$_a$). They indicated that the distribution of "CSWr$_a$" is restricted to depths of 50 and 150 m. However, from the surface to 50 m they attributed to the influence of river discharge (Fig. 1a and 9a). In this work consider that the top 50 m should be included in an analysis that leads to the range of values used for the classification of this water mass. By not including the full range of salinity values, the actual volume of the CSW within the GoM would be underestimated, affect hydrography budgets and, potentially, estimates of productivity. Additionally, in the classification proposed by Portela *et al.* (2018) the overlap in the thermohaline ranges of the CSW and GCW was overlooked (see figure 2 of Portela *et al.*, 2018).

In this work, solved the overlap problem based on the fact that the CSW is closely linked to the LC by the Yucatán Current input to the CB. In this work suggest that the overlap in the characteristics of the CSW and GCW that was not addressed by the Portela *et al.* (2018) classification can be addressed by considering the subsurface DO maximum. Our analysis revealed the existence of a subsurface DO maximum, which allowed us to separate the upper limit of the GCW from the bottom of the CSW. However, in this work suggest that the

https://doi.org/10.5194/bg-2019-340
Preprint. Discussion started: 23 September 2019

mechanism by which do behaves conservatively is as follows: during autumn-winter when the incursion of LC is minimal, the GCW is distributed at the surface. Intense winds are known as "Nortes" occur during this period and intense mixing takes place in surface waters of the GCW, resulting in the homogenization of all properties. The oxygen concentration measured during the winter months was approx. 220 $\mu mol \cdot kg^{-1}$ (Fig. 6a-b and 7c). During spring-summer, the LC advects the warm, oligotrophic waters of the CSW into the interior of the GoM on top of the GCW. This water has a lower DO concentration than that found in the surface waters of GCW in winter, which is caused by temperature-related differences in solubility (Benson and Krause, 1984). The warm water of the CSW induces stratification that limits the exchange of oxygen with the underlying GCW (Fig. 6a-c, 7a, and 7c). The boundary between both water masses is therefore indicated by the maximum subsurface DO concentration (Fig. 6). In this work estimate that the DO concentration difference is approx. 50 $\mu mol \cdot kg^{-1}$ (180 to 230 $\mu mol \cdot kg^{-1}$ see figure 6), and can this difference can be explained by differences in solubility, ruling out that the DO maximum is associated with photosynthesis. This is supported by a depth difference between the peak of maximum fluorescence and the maximum subsurface DO, maximum fluorescence occurs below of the subsurface DO maximum (Supplementary Fig. 3). Also, during summer cruises, the AOU in the CSW tends towards negative values (Supplementary Fig. 1c-e), these are usually found above densities of approx. 24 $kg \cdot m^{-3}$ (Fig. 5), from a greater exchange with the atmosphere. In contrast, during late autumn and winter, the AOU presented positive values due to more respiration within the GCW (Supplementary Fig. 1a-b).

4. 1. 2. On the formation of GCW

The surface presence of the GCW in the autumn and winter is caused by: 1) the absence of CSW due to the retraction of the LC, and 2) the strong winds that result in a well-defined and deep (100 m) mixed layer. This last observation was previously pointed out by Nowlin and MCLellan (1967), Elliott (1979,1982), Vidal *et al*. (1994), and Portela *et al*. (2018). It has been suggested that the formation of the GCW originates from the erosion of the SUW (Vidal *et al*., 1992, 1994; Portela *et al*., 2018). However, our results suggest GCW formation originates from the mixture of the remains of CSW and SUW within the GoM when the LC is retracted. During fall and winter, the remnant of these water masses in the interior of the gulf is mixed with TACW to form GCW.

During winter, when the CSW is absent, the TACW was also shallower than in summer. The proximity of the TACW to the GCW facilitates the vertical exchange of chemical properties towards the surface. Convective mixing leads to low DO concentrations of the TACW to be reflected in the GCW, as well as causing an observable increase in nitrate and DIC concentrations (Fig. 6). Furthermore, observations by satellite of the GoM found maximum concentrations of chlorophyll in winter (Pasqueron *et al*., 2017). This is in agreement with Damien *et al*. (2018), who found a winter chlorophyll concentration increase explained by the amount of nutrient injected into the euphotic layer by the dynamic of the winter mixed-layer.

4. 1. 3. Freshwater Influenced Surface Water (FISW)

The presence of FISW reported in this study during the summers in the central region (24º-25ºN, 95.6º-88ºW) is likely due to river inflows, precipitation and offshore transport. In the central region of the GoM, relatively low salinities were measured that can only be explained by the contribution of freshwater from rivers or precipitation. For example, in the central stations located along 25 ºN, salinities of approximately 33.1 were detected in the first 20 m of the water column, which would lead to the formation of FISW (Fig. 1c). These freshwater inputs were also reported by Portela *et al*. (2018), who detected the influence of low salinity waters (33 $g \cdot kg_{-1}$) within the first 50 m in the central gulf. These low salinities have been attributed to the influence of freshwater inflow from rivers to the continental shelf in the northern GoM and transport to the central gulf by anticyclonic eddies; hence, low surface salinities can be found hundreds of kilometers from the river source (Morey *et al*., 2003a; Morey *et al*., 2003b; Jochens & DiMarco, 2008, Brokaw *et al*., 2019).

In the northern GoM, the Mississippi and Atchafalaya rivers flow into the GoM. Their outflow is generally transported westward along the Louisiana shelf during the summer months (Cochrane and Kelly, 1986; Ohlmann and Niiler, 2005; Smith and Jacobs, 2005) in response to predominant winds from the north and east (Wang *et al*., 1998). Besides, it has been reported that these rivers have their highest inflow during the spring/summer (Morey *et al*., 2003a).

In the southern GoM the Tonalá, Coatzacoalcos, and Usumacinta rivers flow into the region bordering CB. It has been reported that the propagation of low salinity filaments can be caused by local circulation resulting in a salinity gradient from coast to ocean (Vidal *et al*., 1994). In this work also observed the FISW as part of a salinity gradient of 35.4 to 36.3 that extended from the edge of the shelf toward the ocean, particularly during the winter. Also, a decrease in offshore salinity was attributed in the coastal region of the CB to freshwater input by Vidal *et al*. (1994); FISW was also detected at stations closer to the coastal region of the CB in the three summers oceanographic camping. It may also be noted that this type of water

https://doi.org/10.5194/bg-2019-340
Preprint. Discussion started: 23 September 2019

was observed in the semi-permanent cyclonic eddy reported by Nowlin (1972) and Pérez-Brunius *et al*. (2013), which could contribute to the transport of the FISW in the Campeche region during both summer and winter.

Concerning the biogeochemical role of the FISW in the surface waters within the GoM, the following questions remain: 1) what is its influence of the FISW in the first 20 m? and 2) what is its influence in the central GoM?

These questions highlight the need to carry out studies of biogeochemical processes at smaller scales to determine their role within the GoM. Undoubtedly, it is also important to carry out studies at the river mouths to determine the flow of nutrients and organic matter to the gulf.

4. 1. 4. The surface water masses modulate the depth of the nutricline

One of the biological implications of the presence of CSW is that it is oligotrophic reaching down to 90 m in spite. This can be seen in figure 10, wherein this work compares the vertical distribution of nitrate and density with ADT maps for summer 2015 (when mesoscale eddies were abundant) and winter 2013 (when the number and spatial extent of eddies were smaller). During summer, a near-surface incursion of low-density water associated with the CSW was observed (white line Fig. 10a). This incursion brought water with oligotrophic characteristics to depths shallower than 70 m (nitrate from 0 to 0.48 μM; DIC H 1978 μmol·kg$_{-1}$, Fig. 8). Nitrogen fixation process uses to be present on this oligotrophic surface North Atlantic Ocean

https://doi.org/10.5194/bg-2019-340
Preprint. Discussion started: 23 September 2019

waters (Montoya *et al*., 2002). The horizontal distribution of the concentration of nitrate and DIC was reduced by stratification following the entrance of the LC that transport the CSW into the interior of the gulf. In winter, the absence of the CSW is accompanied by a well-mixed density distribution in the first 200 m as the GCW predominates (Fig. 10d). Higher nitrate (0.02 to 13.7 μM) and carbon (> 2036 $\mu mol \cdot kg^{-1}$) concentrations were observed near the surface above depths 75 m.

Therefore, the alternating absence or presence of the CSW is related to the nutricline depth; in summer when CSW overlies the GCW, the nutricline is deepest (Fig. 10). In winter, when the GCW predominates and the TACW is shallower, deeper and well-defined, the nutricline is found closer to the surface. The importance of this redefinition of the water masses contributes to a better understanding of their role in the dynamics of nutrients (and carbon). Finally, an analysis was carried out using the CARS2009 database (CSIRO Atlas of Regional Seas) in order to evaluate the temporal changes of the CSW and the GCW. Figure 11 contrasts climatological averages between winter (February) and summer (July). The T_θ-S diagram, as well as the vertical sections, show that CSW is only evident during the summer while during the winter only the GCW is detected from the surface to approximately 200 m deep. This supports our suggestion that the seasonal extension and retraction of the LC favors the formation of the subsurface maximum of DO during the summer and disappears in winter. Figure 11 shows that during the presence of the CSW cause a deepening of the nutricline during the summer to H 150 m in contrast to winter when the nutricline rises toH100 m.

The analysis of the CARS2009 climatological data confirms the importance of CSW in affecting the near-surface biogeochemical characteristics of the GoM. Both the cruise data

https://doi.org/10.5194/bg-2019-340
Preprint. Discussion started: 23 September 2019

and the CARS2009 climatological data sets affirm that the DO subsurface maximum can be used to define the upper limit of the GCW. During the summer months, with the entry of LC and dissipation by eddies, the presence of CSW dominates in the first 100 m, potentially having an impact on the primary productivity of the GoM, as indicated throughout this work and by other authors (Nowlin & McLellan, 1967; Tanahara, 2004; Schmitz, 2005; Delgado *et al*., 2019),

5. Conclusions.

A re-classification of the water masses above the 26 kg·m-3 isopycnal was carried out resulting in a modification of the present thermohaline ranges defining the CSW and GCW water masses. For the re-classification of the CSW and the GCW, DO concentrations were a key indicator of water mass limits. In addition, another water mass, the FISW, formed by the influence of the freshwater inputs, was included in the new classification.

CSW was detected only during the summer with a vertical spatial domain encompassing the first 90 m and featured warm waters, high salinities, non-detectable nitrate concentration, and negative values of the AOU. It was also found that the lower limit of this water mass is delimited by a maximum subsurface DO. The presence of this subsurface maximum was found only in the summer and separates the CSW from the GCW. Likewise, the presence and absence of CSW was found to modulate the depth of the nutricline and likely influences primary productivity.

In winter, the replacement of the CSW by the GCW affected the biogeochemical composition of surface water, specifically with an increase in nitrate concentrations, positive values of AOU and a decrease in surface temperatures. The TACW lies below the GCW and is closer

https://doi.org/10.5194/bg-2019-340
Preprint. Discussion started: 23 September 2019

to the surface than during the summer, contributing to nutrient availability and low DO near the surface.

The SUW was detected during most of the year only in the vicinity of the Yucatán Channel and along the region of influence of the LC. This mass of water stands out for its subsurface salinity maximum, low DO and high nitrate and DIC concentrations when compared to CSW.

Finally, in this work proposed new criteria for the identification of the near-surface FISW. This was detected in the central oceanic region of the GoM indicating the contribution of precipitation and offshore transport of river discharge waters from the northern GoM (Mississippi and Atchafalaya).

Data availability

The data is not available at the moment.

Author contribution

The study was conceived by all co-authors. GYCD carried out the sampling on board *R/V Justo Sierra* cruise XIXIMI-1 to XIXIMI-5 and the analytical work in the laboratories at the Oceanological Research Institute (IIO) México. This work proposes a new reclassification of the surfaces water masses in the GoM for the long-term effects on conditions biogeochemical processes. GYCD prepared the manuscript with substantial contributions from all co-authors.

Competing interest

https://doi.org/10.5194/bg-2019-340
Preprint. Discussion started: 23 September 2019

Biogeosciences Discussions

The authors declare that they have no conflict of interest.

6. Acknowledgements

This study is a contribution of the Consorcio de Investigación del Golfo de México (CIGoM) through the project 201441 "Implementación de redes de observación oceanográficas (físicas, geoquímicas, ecológicas) para la generación de escenarios ante posibles contingencias relacionadas a la exploración y producción de hidrocarburos en aguas profundas del Golfo de México" funded by Secretary of Energy (SENER)-National Council of Science and Technology of Mexico (CONACyT) Hydrocarbons Fund. Altimeter products were produced by Data Unification and Altimeter Combination System available on the AVISO (Archiving, Validation and Interpretation of Satellite Oceanographic data) https://www.aviso.altimetry.fr/en/data. Wind Stress, Geostrophic and Ekman Currents were extracted from GEKCO (Geostrophic Ekman Current Observatory, Sudre et al., 2013) http://www.legos.obs-mip.fr/members/sudre/gekco_form with support from LEGOS. In particular for wind stress GEKCO product, they were used these three sources for 01/01/1993 - 27/10/1999 period https://www.ncdc.noaa.gov/data-access/marineocean-data/blended-global/blended-sea-winds, for 28/10/1998 - 20/03/2007 period (MWF L3 daily QuikSCAT product) http://cersat.ifremer.fr and for the 21/03/2007 - 31/12/2017 period (MWF L3 daily ASCAT product) http://cersat.ifremer.fr/data/products/catalogue. Finally, the general features of the Gulf of Mexico Loop Current eddies were taken from https://www.horizonmarine.com/loop-current-eddies. Also, we especially thank Dra. Esther Portela her positive criticisms and suggestions.

References

Benson, B.B., and D. Krause.: The concentration and isotopic fractionation of oxygen dissolved in freshwater and seawater in equilibrium with the atmosphere. *Limnology and Oceanography* 29 (3): 620–632. 1984.

Biggs, D. C., & Ressler, P. H.: Distribution and abundance of phytoplankton, zooplankton, ichthyoplankton, and micronekton in the deepwater Gulf of Mexico. Gulf of Mexico. *Science,* 2001(1), 7–29. http://doi.org/10.18785/goms.1901.02. 2001.

Brokaw, R. J., Subrahmanyam, B., & Morey, S. L.: Loop current and eddy-driven salinity variability in the Gulf of Mexico. Geophysical Research Letters, 46. https://doi.org/10.1029/ 2019

Bunge, L., Ochoa, J., Badan, A., Candela, J., and Sheinbaum, J.: Deep flows in the Yucatan Channel and their relation to changes in the Loop Current extension, J. Geophys. Res., 107, C12, https://doi.org/10.1029/2001JC001256. 2002.

Carrillo, L, Johns, E. M., Smith, R. H., Lamkin, J. T., & Largier, J. L.: Pathways and hydrography in the Mesoamerican Barrier Reef System Part 2: Water masses and thermohaline structure. *Continental Shelf Research,* 120, 41–58. http://doi.org/10.1016/j.csr.2016.03.014. 2016.

Cochrane, J. D., and E J. Kelly.: Low-frequency circulation on the Texas-Louisiana continental shelf, *J. Geophys. Res*., 91 (C9), 10,645- 10,659. 1986.

https://doi.org/10.5194/bg-2019-340
Preprint. Discussion started: 23 September 2019

Biogeosciences Discussions

Delgado, J. A., Sudre, J., Tanahara, S., Montes, I., Hernandez-Ayon, J. M., and Zirino, A.: Effect of Caribbean Water Incursion into the Gulf of Mexico derived from Absolute Dynamic Topography, Satellite Data, and Remotely – sensed Chlorophyll-*a*, *Ocean Sci. Discuss.,* https://doi.org/10.5194/os-2019-58, in review, 2019.

Damien, P., Pasqueron de Fommervault, O., Sheinbaum, J., Jouanno, J., Camacho-Ibar, V. F., & Duteil, O.: Partitioning of the Open Waters of the Gulf of Mexico Based on the Seasonal and Interannual Variability of Chlorophyll Concentration. *Journal of Geophysical Research: Oceans*, 123(4), 2592–2614. http://doi.org/10.1002/2017JC013456. 2018.

Dickson, A.G., Sabine, C.L. & Christian, J.R.: Guide to Best Practices for Ocean CO2 Measurements, *PICES Special Publication.* 2007.

Elliott, B. A.: Anticyclonic rings and the energetics of the circulation of the Gulf of Mexico. *Ph.D. Dissertation, Texas A & M Univ., College Station, Texas*. 1979.

Elliott, B. A.: Anticyclonic Rings in the Gulf of Mexico. *Journal of Physical Oceanography.* 1982.

Gallegos, A.: Descriptive physical oceanography of the Caribbean Sea. Small Islands: Marine Science and Sustainable Development Coastal and Estuarine Studies 51. *American Geophysical Union, United States, pp*. 36–55. 1996.

El-Sayed, S. Z.: Primary productivity and standing crop of phytoplankton, in: Chemistry, primary productivity, and benthic algae of the Gulf of Mexico, edited by: Bushnell, V. C., 8–13 pp., *American Geographical Society, New York*. 1972.

https://doi.org/10.5194/bg-2019-340
Preprint. Discussion started: 23 September 2019

Biogeosciences Discussions

Hall, C. A. and R. R. Leben.: Observational evidence of seasonality in the timing of Loop Current eddy separation. *Dyn. Atmos. Oceans*, 76, 240–267, https://doi.org/10.1016/j.dynatmoce.2016.06.002. 2016.

Hamilton, P.: Eddy statistics from Lagrangian drifters and hydrography for the northern Gulf of Mexico slope, *J. Geophys. Res.,* 112, C9, https://doi.org/10.1029/2006JC003988. 2007a.

Hamilton, P., R. Leben, A. Bower, H. Furey, and P. Pérez-Brunius.: Hydrography of the Gulf of Mexico using autonomous floats. *J. Phys. Oceanogr.,* 48, 773–794, https://doi.org/10.1175/JPO-D-17-0205.1. 2018.

Heileman, S., & Rabalais, N.: XV-50 Gulf of Mexico: LME# 5. The UNEP Large Marine Ecosystem Report. A perspective on the changing condition in LMEs of the world's Regional Seas. *UNEP Regional Seas Report and Studies,* (182). 2009.

Herring, J.H.: Gulf of Mexico hydrographic climatology and method of synthesizing subsurface profiles from the satellite sea surface height anomaly. US. Department of Commerce. National Oceanic and Atmospheric Administration. National Ocean Service. Coastal Survey Development Laboratory. Report 122, 63 pp. 2010.

Hernández-Guerra, A., & Joyce, T. M.: Water masses and circulation in the surface layers of the Caribbean at 66 W. Geophysical research letters, 27(21), 3497-3500. https://doi.org/10.1029/1999GL011230 . 2000

https://doi.org/10.5194/bg-2019-340
Preprint. Discussion started: 23 September 2019

Hydes DJ, Aoyama M, Aminot A, Bakker K, Becker S, Coverly S, Daniel A, Dickson AG, Grosso O, Kerouel R, van Ooijen J, Sato K, Tanhua T, Woodward EMS, Zhang JZ.: Determination of dissolved nutrients (N, P, Si) in seawater with high precision and inter-comparability using das-segmented continuous flow analyzers. *In: Hood EM, Sabine CL, Sloyan BM (eds) The GO-SHIP repeat hydrography manual: a collection of expert reports and guidelines, IOCCP report number 14, ICPO publication series number 134, UNESCO-IOC, Paris, France*. http://www.go-ship.org/HydroMan.html. 2010.

Jochens, A. E., & DiMarco, S. F.: Physical oceanographic conditions in the deepwater Gulf of Mexico in summer 2000–2002. *Deep-Sea Research Part II: Topical Studies in Oceanography,* 55(24–26), 2541–2554. https://doi.org/10.1016/j.dsr2.2008.07.003. 2008.

Johnson, K. M., P. J. Williams, L. Brändström, and J. M. Sieburth.: Coulometric TCO2 analysis for marine studies: Automation and calibration, *Mar. Chem*., 21, 117–133, https://doi.org/10.1016/0304-4203(87)90033-8 1987.

Linacre, L., Lara-Lara, R., Camacho-Ibar, V., Herguera, J. C., Bazán-Guzmán, C., & Ferreira-Bartrina, V.: Distribution pattern of picoplankton carbon biomass linked to mesoscale dynamics in the southern Gulf of Mexico during winter conditions. *Deep Sea Research Part I: Oceanographic Research Papers,* 106, 55-67. 2015.

Martínez-López B. and J. Zavala-Hidalgo.: Seasonal and interannual variability of cross-shelf transports of chlorophyll in the Gulf of Mexico. *J Mar Syst*. **77**, 1-20. 2009.

https://doi.org/10.5194/bg-2019-340
Preprint. Discussion started: 23 September 2019

Biogeosciences Discussions

McDougall, T. J., & Barker, P. M.: Getting started with TEOS-10 and the Gibbs Seawater (GSW) *Oceanographic Toolbox.* (SCOR/IAPSO WG127, Ed.). 2011.

Merrell, W. J., & Morrison, J. M.: On the circulation of the western Gulf of Mexico with observations from April 1978. *Journal of Geophysical Research,* 86(C5), 4181–4185. https://doi.org/10.1029/JC086iC05p04181. 1981.

Montoya, J., E. Carpenter, and D. Capone.: Nitrogen fixation and nitrogen isotope abundance in zooplankton of the oligotrophic North Atlantic, *Limnol. Oceanogr.*, 47, 1617–1628. https://doi.org/10.4319/lo.2002.47.6.1617. 2002.

Morrison, J. M., Merrel, W. J., Key, R. M., & Key, T. C.: Property distributions and deep chemical measurements within the western Gulf of Mexico. *Journal of Geophysical Research*, 88(C4), 2601–2608. https://doi.org/10.1029/JC088iC04p02601. 1983.

Morey, S. L., Martin, P. J., O'Brien, J. J., Walclraft, A. A., & Zavala-Hidalgo, J.: Export pathways for river discharged fresh water in the northern Gulf of Mexico. *Journal of Geophysical Research*, 108(C10), 3303. https://doi.org/10.1029/2002JC001674. 2003a.

Morey, S. L., Schroeder, W. W., O'Brien, J. J., & Zavala-Hidalgo, J.: The annual cycle of riverine influence in the eastern Gulf of Mexico basin. *Geophysical Research Letters*, 30(16), 1–4. http://doi.org/10.1029/2003GL017348. 2003b.

Müller-Karger, F. E., Smith, J. P., Werner, S., Chen, R., Roffer, M., Liu, Y., B. Muhling, D. Lindo-Atichati, J. Lamkin, S. Cerdeira-Estrada, D.B. Enfield.: Natural variability of surface oceanographic conditions in the offshore Gulf of Mexico. *Progress in Oceanography*, 134, 54–76. https://doi.org/10.1016/j.pocean.2014.12.007. 2015.

Nowlin, W. D. and MCLellan, H. J.: A characterization of Gulf of Mexico waters in winter, *J. Mar. Res*., 25, 1292–1309. 1967.

Nowlin, W. D. Jr.: Winter circulation patterns and property distributions. In: Contributions on the Physical Oceanography of the Gulf of Mexico, *Texas A & M University Oceanographic Studies. Eds. L. R. A. Capurro and J. L. Reid*, 2, 3-51. 1972.

Nowlin, W. D., Jr., A. E. Jochens, S. F. DiMarco, R. O. Reid, and M. K. Howard.: Deepwater Physical Oceanography Reanalysis and Synthesis of Historical Data: Synthesis Report. OCS Study MMS 2001- 064, *U.S. Dept. of the Interior, Minerals Management Service, Gulf of Mexico OCS Region, New Orleans, LA*. 530 pp. 2001.

Ohlmann, J.C., Niiler, P.P.: Circulation over the continental shelf in the northern Gulf of Mexico. *Prog. Oceanogr*. 64 (1), 45–81. 2005.

Pasqueron De Fommervault, O., Pérez-Brunius, P., Damien, P., Camacho-Ibar, V. F., & Sheinbaum, J.: Temporal variability of chlorophyll distribution in the Gulf of Mexico: Bio-optical data from profiling floats. *Biogeosciences*, 14(24), 5647–5662. http://doi.org/10.5194/bg-14-5647-2017. 2017.

https://doi.org/10.5194/bg-2019-340
Preprint. Discussion started: 23 September 2019

Pérez-Brunius, P., García-Carrillo, P., Dubranna, J., Sheinbaum, J., and Candela, J.: Direct observations of the upper layer circulation in the southern Gulf of Mexico. *Deep Sea Res. Part II: Topical Studies in Oceanography,* 85, 182-194. https://doi.org/10.1016/j.dsr2.2012.07.020. 2013.

Portela, E., Tenreiro, M., Pallàs-Sanz, E., Meunier, T., Ruiz-Angulo, A., Sosa-Gutiérrez, R., & Cusí, S.: Hydrography of the central and western Gulf of Mexico. *Journal of Geophysical Research: Oceans*, 1–16. http://doi.org/10.1029/2018JC013813. 2018.

Rivas, D., Badan, A., & Ochoa, J.: The ventilation of the deep Gulf of Mexico. *Journal of Physical Oceanography*, 35(10), 1763–1781. https://doi.org/10.1175/JPO2786.1. 2005.

Smith, S.R., Jacobs, G.A. (2005). Seasonal circulation fields in the northern Gulf of Mexico caclulated by assimilating current meter, shipboard ADCP, and drifter data simultaneously with the shallow water equations. Cont. Shelf Res. 25 (2), 157–183.

Sturges, W. and Leben, R.: Frequency of ring separations from the Loop Current in the Gulf of Mexico: A revised estimate, *J. Phys. Oceanogr.*, 30, 1814–1819. DOI: 10.1175/1520-0485(2000)030<1814:FORSFT>2.0.CO;2. 2000.

Schmitz Jr. W. J., D. C. Biggs, A. Lugo-Fernandez, L.-Y. Oey, W. Sturges: A synopsis of the circulation in the Gulf Of Mexico and on its continental margins. *Circulation in the Gulf of Mexico: Observations and Models. (2005), Geophys. Monogr. Ser., vol. 161,*

https://doi.org/10.5194/bg-2019-340
Preprint. Discussion started: 23 September 2019

edited by W. Sturges and A. Lugo-Fernandez, pp. 11-29, AGU, Washington, D. C. https://doi.org/*10.1029/161GM03.* 2005.

Tanahara, S.: Étude de la circulation dans le Golfe du Mexique et la Mer des Caraïbes. Validation des simulations CLIPPER-ATL6 à l'aide des observations CANEK. *Doctoral dissertation, Sciences de la Terre et de l'Univers, Université Paris VI, Paris, France*, 2004.

Vidal, V. M. V, Vidal, F. V, & Pérez-Molero, J. M.: Collision of a loop current anticyclonic ring against the continental shelf slope of the western Gulf of Mexico. *Journal of Geophysical Research: Oceans,* 97(C2), 2155–2172. http://doi.org/10.1029/91JC00486. 1992.

Vidal, V. M. V., Vidal, F. V., Hernández, A. F., Meza, E., & Zambrano, L.: Winter water mass distributions in the western Gulf of Mexico affected by a colliding anticyclonic ring. *Journal of Oceanography*, 50(5), 559–588. http://doi.org/10.1007/BF02235424. 1994.

Wang, W., Nowlin, W.D., Reid, R.O.: Analyzed surface meteorological fields over the northwestern Gulf of Mexico for 1992–94: seasonal, and monthly patterns. Mon. *Weather Rev.* 126 (11), 2864–2883. DOI:10.1175/1520-0493(1998)126%3C2864:ASMFOT%3E2.0.CO;2. 1998.

Wüst, G.: Stratification and circulation in the Antillean-Caribbean basins, *vol. 1, Columbia University Press.* 1964.

Zavala-Hidalgo, J., Romero-Centeno, R., Mateos-Jasso, A., Morey, S. L., & Martínez-López,

https://doi.org/10.5194/bg-2019-340
Preprint. Discussion started: 23 September 2019

B.: The response of the Gulf of Mexico to wind and heat flux forcing: What has been learned in recent years. *Atmosphere*, 27(3), 317–334. https://doi.org/10.1016/S0187-6236(14)71119-1 2014.

https://doi.org/10.5194/bg-2019-340
Preprint. Discussion started: 23 September 2019

Appendix A: Description of the code that was developed in Matlab.

The code developed in Matlab (ver. R2014a) uses a step scheme in which the complete data set is initially included, which will automatically exclude with specific criteria (Table 1) the four structures identified as follows.

This program was developed in the following manner:

1.- Specific criteria were assigned to the thermohaline variables (σ_θ, T_θ, S) and to the DO variable to facilitate the identification and separation of profiles (Table 1).

2.- The program identified hydrographic profiles with similar thermohaline characteristics (previously specified) and grouped them into four data subsets. Each data subset corresponded to one of the previously identified structures. As was observed, the structures associated with SUW (1st pattern; blue: maximum subsurface S; Fig. 4) and FISW (2nd pattern; pink: low surface S; Fig. 4) presented extreme thermohaline characteristics, making them easy to group. However, the structures associated with CSW (3rd pattern; green: maximum surfaces S and T; Fig. 4) and GCW (4th pattern; red: narrow surfaces S and low T; Fig. 4) were more difficult to group, but the DO variable proved to be the key to identification and separation.

3.- To separate the patterns associated with CSW (3rd pattern) and GCW (4th pattern), two additional conditions within the program were set and are as follows:

> **3.1.** To separate CSW from GCW, DO data located between the 23.75 and 24.75 $kg{\cdot}m^{-3}$ isopycnal were averaged (1st condition), associated with the red profile (fourth pattern).

https://doi.org/10.5194/bg-2019-340
Preprint. Discussion started: 23 September 2019

3.2. The code calculated the average value of the DO data less than the 23.5 kg·m^{-3} isopycnal (2nd condition), associated with the green profile (third pattern).

3.3. If there are no data less than 23.5 kg·m^{-3} density, the code will search for the first 5 surface data to average value the DO and carry out the next step (2nd condition).

3.4. Finally, the program carried out a comparison between the average values obtained from both conditions. This comparison was used to determine if the DO values from the 1st condition were greater than those from the 2nd condition. If this was true, the code classified the data set with the green profile characteristics (3rd pattern). If it was not the case, the code classified it with the red profile characteristics (4th pattern).

3.5. After we obtained the four structures separately, they were plotted separately and associated with the water masses present upper the 400 m of the water column. Subsequently, the limits thermohaline properties, DO concentrations, DIC, and nitrates for each identified mass of water were identified.

https://doi.org/10.5194/bg-2019-340
Preprint. Discussion started: 23 September 2019

Biogeosciences
Discussions
Open Access
EGU

Table 1. Thermohaline characteristics and oxygen values used to separate the four identified structures (1st blue pattern; 2nd pink pattern; 3rd green pattern, and 4th red pattern) that were used in the program developed in Matlab (ver. 2014Ra).

T_θ-S patterns	σ_0 (kg m^{-3})	Salinity (S)	Temperature (ºC)	Oxygen (µmol kg^{-1})
Maximum subsurface S (1st)	25.4 - 26	S ≥ 36.68	19 - 22	140 - 160
Low surface S (2nd)	21 - 24	≤ 36.0	24 - 31	O_2 ≥ 193
Maximum surface S and T (3st)	24.8 - 25.25	36.4 - 36.6	22.9 - 23.2	O_2 ≥ 185
Maximum surface S and low T (4th)	23.7 - 24.7	36.3 - 36.67	23.7 - 27.5	190 - 204

Table 2. General characteristics of the new classification of the surface water masses identified based on thermohaline variables (Potential temperature [ºC] and Salinity [psu]), DO [µmol·kg^{-1}], and AOU [µmol·kg^{-1}]. Also, the variability ranges for DIC [µmol·kg^{-1}], nitrates [µM], and depths as a function of each water mass identified in the deep region of the GoM were included.

Water masses	ID	Temperature θ	Temperature Θ	Salinity psu	Salinity gk·g^{-1}	Oxygen (µmol·kg^{-1})	DIC (µmol·kg^{-1})	Nitrates (µM)	Depth (m)	AOU (µmol·kg^{-1})
Caribean Surface Water	**CSW**	**27 - 32**	**27.1 – 32.1**	**36.0 - 36.8**	**36.18 - 36.98**	**180 - 220**	**1978- 2090**	**0 – 0.50**	**< 90**	**-27 to 2**
Subtropical Underwater	**SUW**	**19 - 26**	**19.1 – 26.1**	**36.6 - 37.0**	**36.78 – 37.18**	**136 - 180**	**2098 - 2156**	**0.06 – 7.10**	**100-250**	**50 to 95**
Gulf Common Water	**GCW**	**20 - 27**	**20.1 – 27.1**	**36.3 - 36.6**	**36.48 – 36.78**	**112 - 232**	**2036 - 2172**	**0.02 - 9.40**	**0-200 Winter 50-200 Summer**	**0 to 90**
Freshwater Influenced Surface Water	**FISW**	**24 - 31**	**24.1 – 31.1**	**≤ 36**	**33.28 – 36.18**	**180 - 220**			**≤ 20**	

https://doi.org/10.5194/bg-2019-340
Preprint. Discussion started: 23 September 2019

FIGURE CAPTIONS:

Figure 1: (a) Distribution of the water masses using the classification system proposed by Portela et al. (2018) using conservative temperature (Θ) vs absolute salinity [S_A g·kg^{-1}], water masses as: Caribbean Surface Water remnant ($CSWr_a$), North Atlantic Subtropical Underwater (NASUW), Gulf Common Water (GCW), Tropical Atlantic Central Water (TACW), $TACWn_a$ (nucleus), Antarctic Intermediate Water (AAIW) and North Atlantic Deep Water (NADW). (b) Θ-S_A vs dissolved oxygen [DO, μmol·kg^{-1}] diagram showing upwards of the isopycnal of the 26 kg·m^{-3} using the Portela et al. (2018) classification. The data from the five cruises from 2010 to 2016 were used to generate the Θ-S diagrams. (c) The coverage area for the stations analyzed (transect delimited in black lines) in the GoM from 2010 to 2016.

Figure 2: Seasonal comparison (late fall-winter (a) and summer (b)) of the Θ-S_A vs. DO [μmol·kg^{-1}] diagrams showing upper waters (< 26 kg·m^{-3}) using classification Portela et al. (2018) considered: $CSWr_a$, NASUW, GCW, and TACW. To generate Θ-S_A vs. DO [μmol·kg^{-1}] diagrams in this work used data from the five cruises where the years 2010-2013 (late fall and winter) were separated from the years 2011, 2105 and 2016 (summer).

Figure 3: A comparison of winter (a) and summer (b) conditions of the variability of the depth of 26 kg·m^{-3} density field in the GoM (in situ hydrographic data collected in February/March 2013 and August/September 2015, respectively)

Figure 4: The Θ-S_A diagram shows the four characteristic patterns like the average considering the five cruises (blue: maximum subsurface S; pink: low surface S; green:

https://doi.org/10.5194/bg-2019-340
Preprint. Discussion started: 23 September 2019

Biogeosciences Discussions

maximum surfaces S and T; and red: maximum surfaces S and low T) identified for the five cruises using the ranges shown in Table 1. The Portela et al. (2018), classification was incorporated into the Θ-S_A diagram to determine if the patterns identified to fit the above classification (water masses: $CSWr_a$, NASUW, GCW, and TACW).

Figure 5: The vertical distribution [250 m] of potential density [kg·m$_{-3}$] and potential temperature [ºC] are shown for the late fall of 2010 (a and f), winter of 2013 (b and g) and summers of 2011 (c and h), 2015 (d and i), and 2016 (e and j). The location of the transect is shown in figure 1c.

Figure 6: The vertical distribution [250 m] of dissolved oxygen [µmol·kg$_{-1}$] are shown for the late fall of 2010 (a), winter of 2103 (b) and summers of 2011 (c), 2015 (d), and 2016 (e). The white contours indicate the lower limit of CSW [24 kg·m$_{-3}$] and GCW [26 kg·m$_{-3}$] in all sections. The location of the transect is shown in figure 1c.

Figure 7: This figure shows the new classification of the water masses with the adjustments to the thermohaline range limits based on the distribution that the four patterns in Figure 2c. (a) The T_θ-S vs DO [µmol·kg$_{-1}$] diagram shows the profiles with SUW characteristics. (b) T_θ-S vs DO [µmol·kg$_{-1}$] diagram presents characteristics particular with SCW (c) T_θ-S vs DO [µmol·kg$_{-1}$] diagram associated with GCW. (d) T_θ-S vs DO [µmol·kg$_{-1}$] diagram associated to the water mass called Freshwater Influenced Surface Water (FISW).

Figure 8: (a) T_θ-S vs nitrate [NO_{2^-} + NO_{3^-}, µM] and (b) T_θ-S vs dissolved inorganic carbon [DIC, µmol·kg$_{-1}$] diagrams corresponding to the winters of 2010 and 2013. (c) T_θ- S vs nitrate

https://doi.org/10.5194/bg-2019-340
Preprint. Discussion started: 23 September 2019

[μM] and (d) T_θ-S vs DIC [μmol·kg^{-1}] corresponding to summer 2015.

Figure 9: Comparison of the classification system proposed by (a) Portela et al. (2018) and (b) this study. Shows the Θ-S_A vs. DO [μmol·kg^{-1}] diagram showing upwards of the isopycnal of the 26 kg·m^{-3} using the reclassification proposed in this work. The names of the water masses used in this work are: Caribbean Surface Water (CSW), Subtropical Underwater (SUW), Gulf Common Water (GCW), and the Freshwater Influenced Surface Water (FISW).

Figure 10: The vertical distribution [250 m] of potential density [kg·m^{-3}] is shown for the summer of 2015 (a) and winter of 2013 (d). The white contours indicate the lower limit of CSW [24 kg·m^{-3}; (a)] and of GCW [26 kg·m^{-3}; (d)] in both sections. The ADT maps show the trajectory of the summer (b) and winter (e) sections of each cruise. The nitrate profiles [μM] (c=summer; f=winter) only include the stations that are found within the trajectory traced in the ADT maps for each cruise. The blue color points indicate the stations that are found outside of the areas influenced by anticyclonic rings while the red color points denote stations located in the area of influence of the anticyclonic gyres.

Figure 11: Θ-S_A vs. DO [μmol·kg^{-1}] annual diagrams from February (a) and July (b) showing the reclassification proposed in this work. Data derived from the CARS-2009 database. Annual vertical sections (-95.5 to -86.5 ºW, 25 ºN; the section shown in figure 1c from the station C to D) of oxygen [μmol·kg^{-1}] concentration and nitrate [μM] for February (c, and d), and July (e, and f) derived from the CARS-2009 database

https://doi.org/10.5194/bg-2019-340
Preprint. Discussion started: 23 September 2019

Biogeosciences Discussions
Open Access

955 **FIGURE 1:**

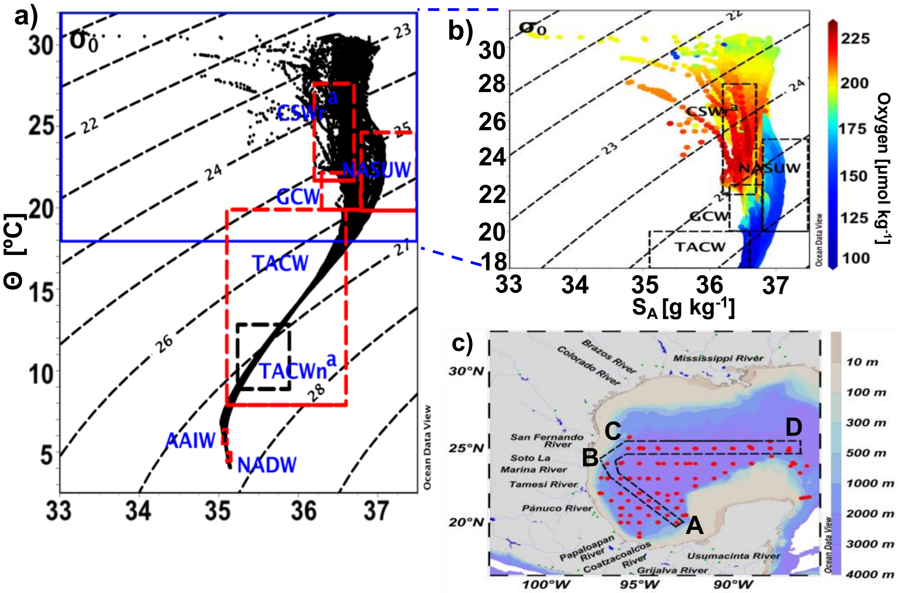

956

957 **FIGURE 2:**

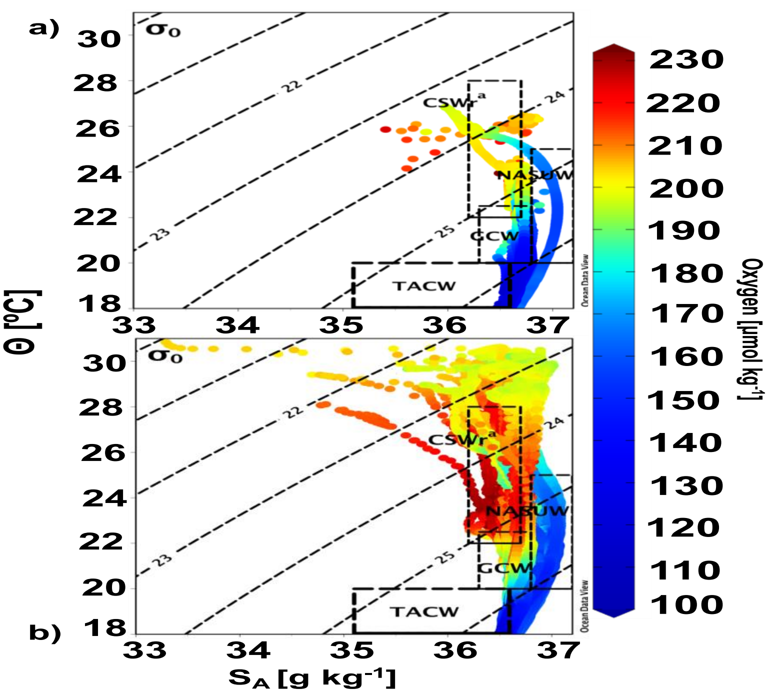

958

https://doi.org/10.5194/bg-2019-340
Preprint. Discussion started: 23 September 2019

FIGURE 3:

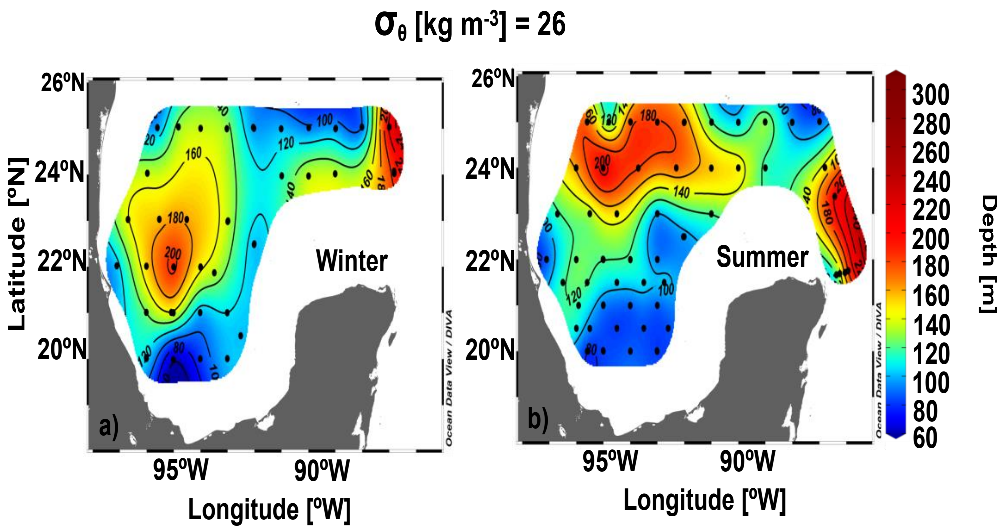

FIGURE 4:

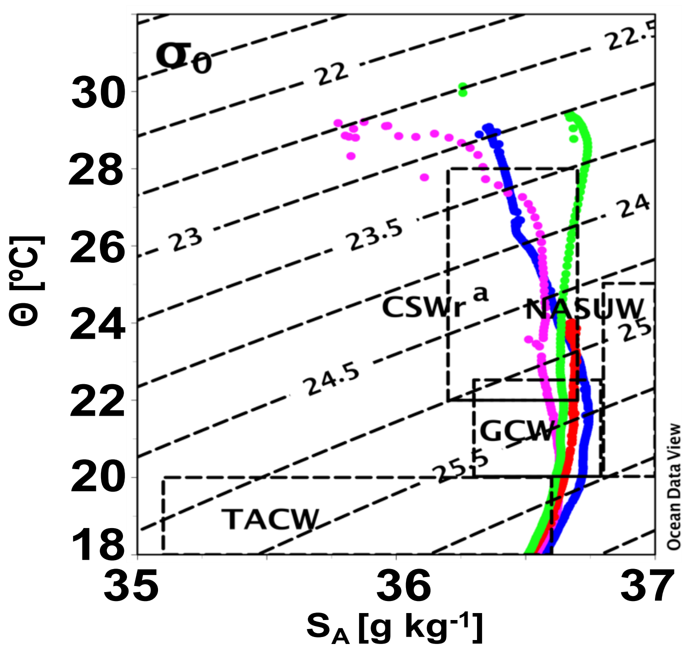

https://doi.org/10.5194/bg-2019-340
Preprint. Discussion started: 23 September 2019

Biogeosciences Discussions

965 **FIGURE 5:**

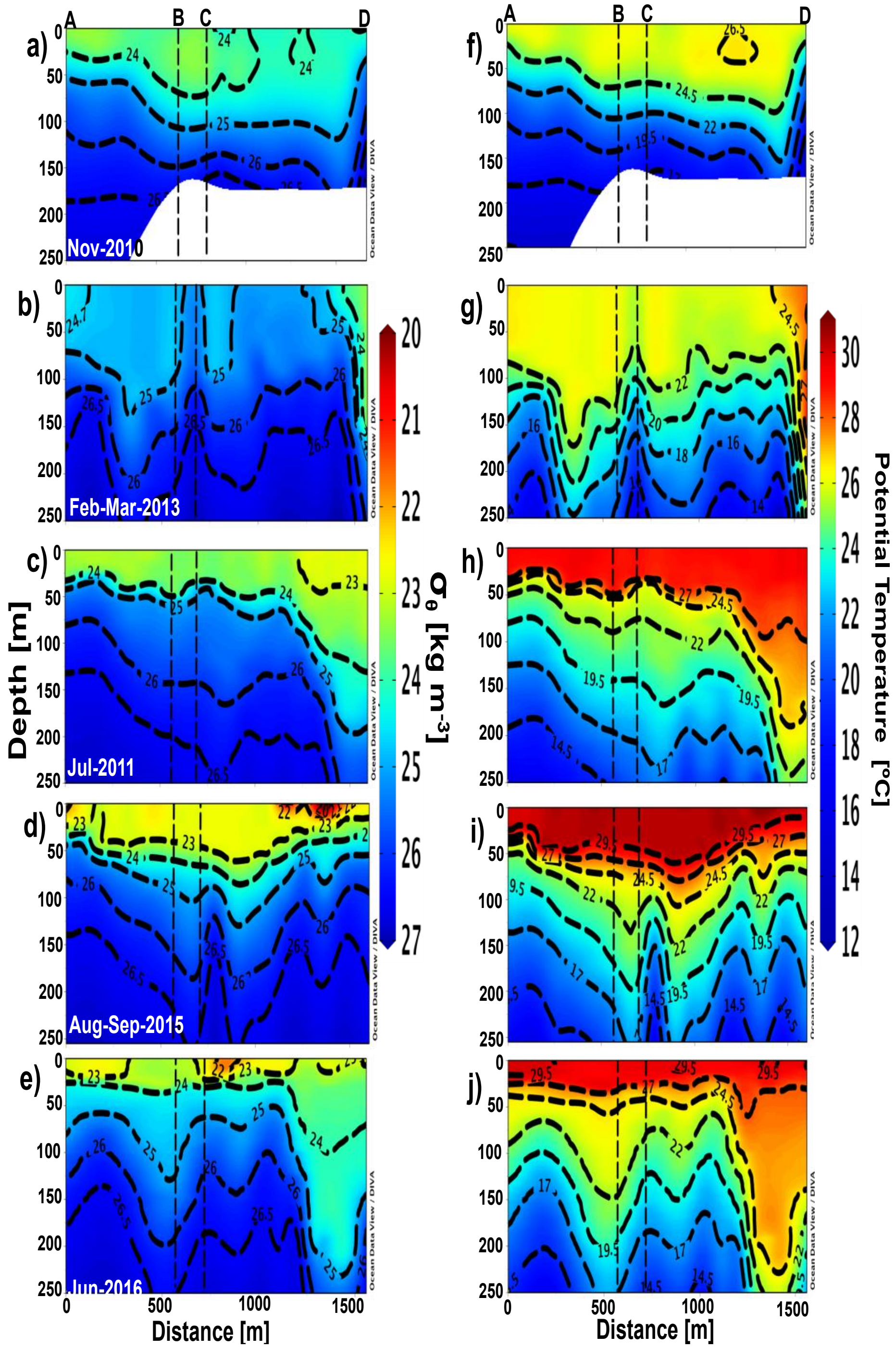

966

https://doi.org/10.5194/bg-2019-340
Preprint. Discussion started: 23 September 2019

FIGURE 6:

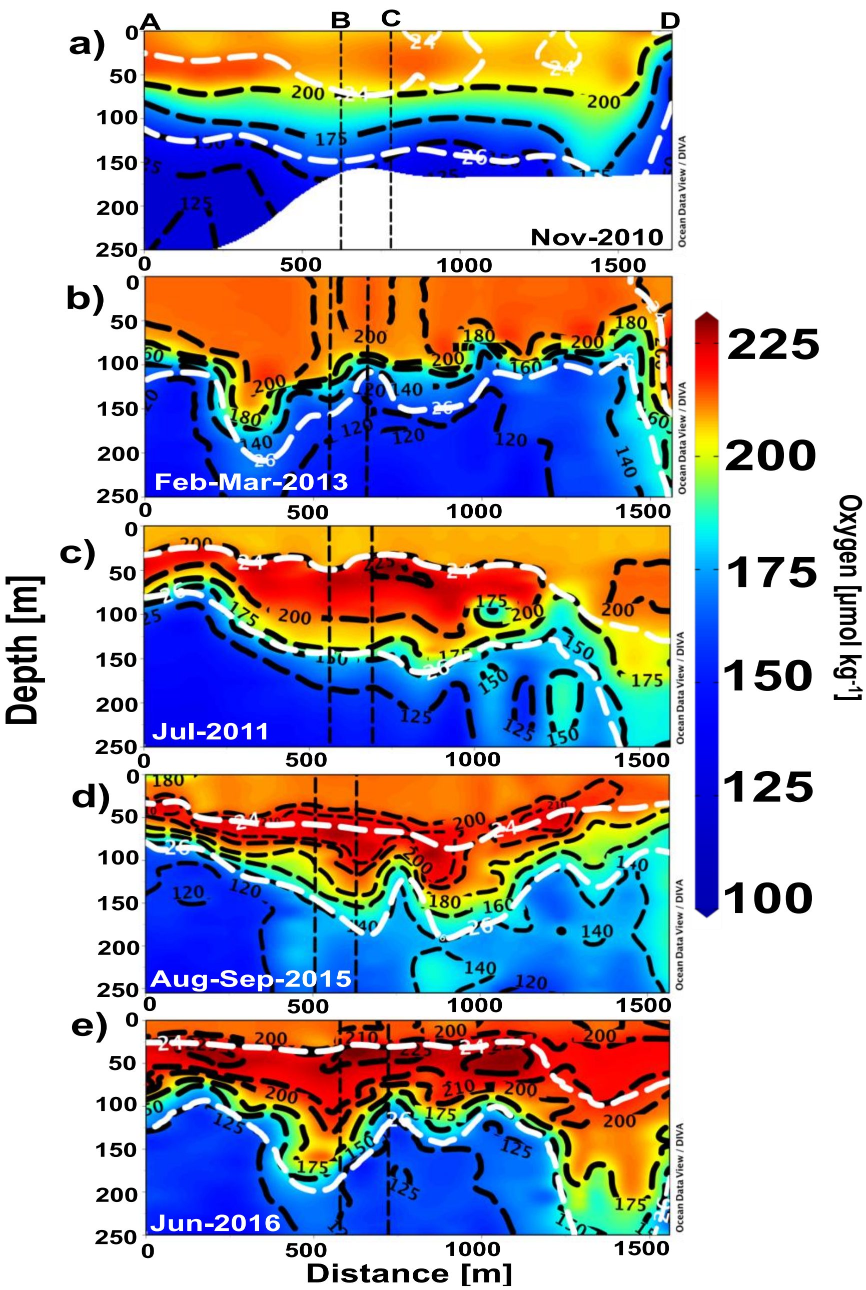

https://doi.org/10.5194/bg-2019-340
Preprint. Discussion started: 23 September 2019

971 **FIGURE 7:**

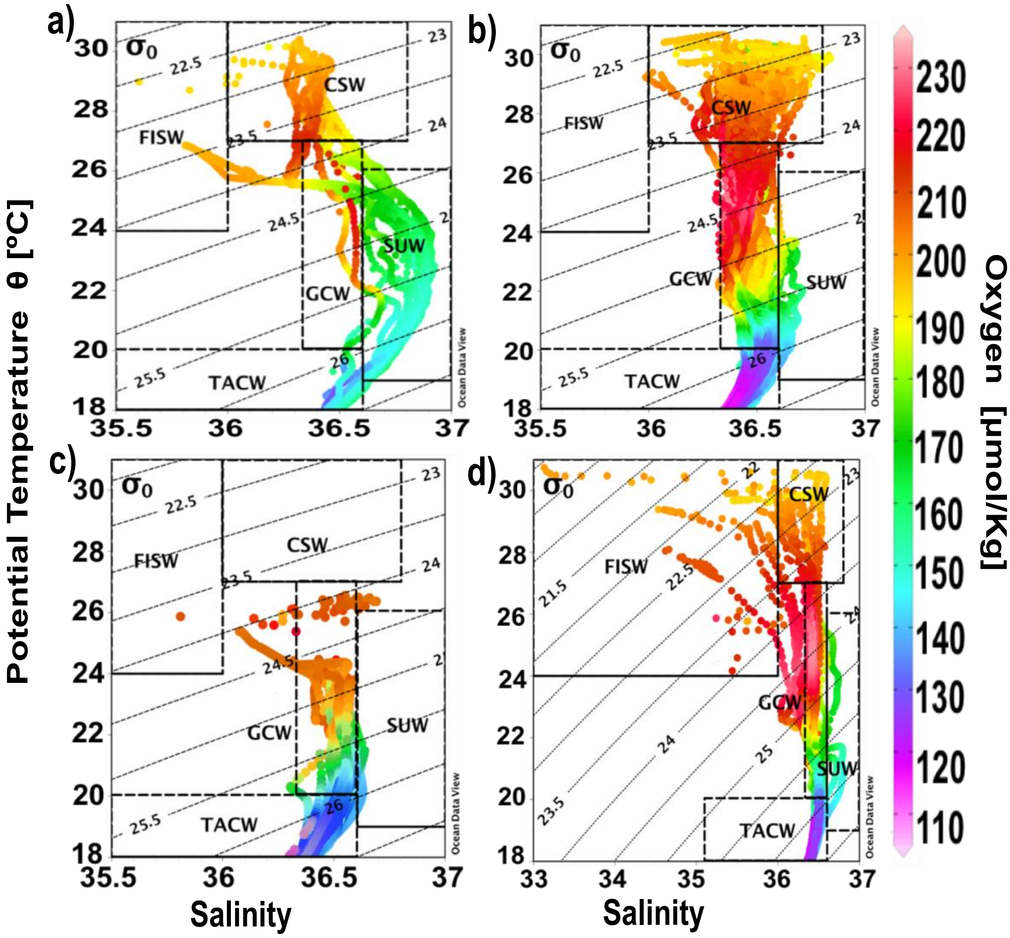

972

973

974

975

976

977

978

979

https://doi.org/10.5194/bg-2019-340
Preprint. Discussion started: 23 September 2019

FIGURE 8:

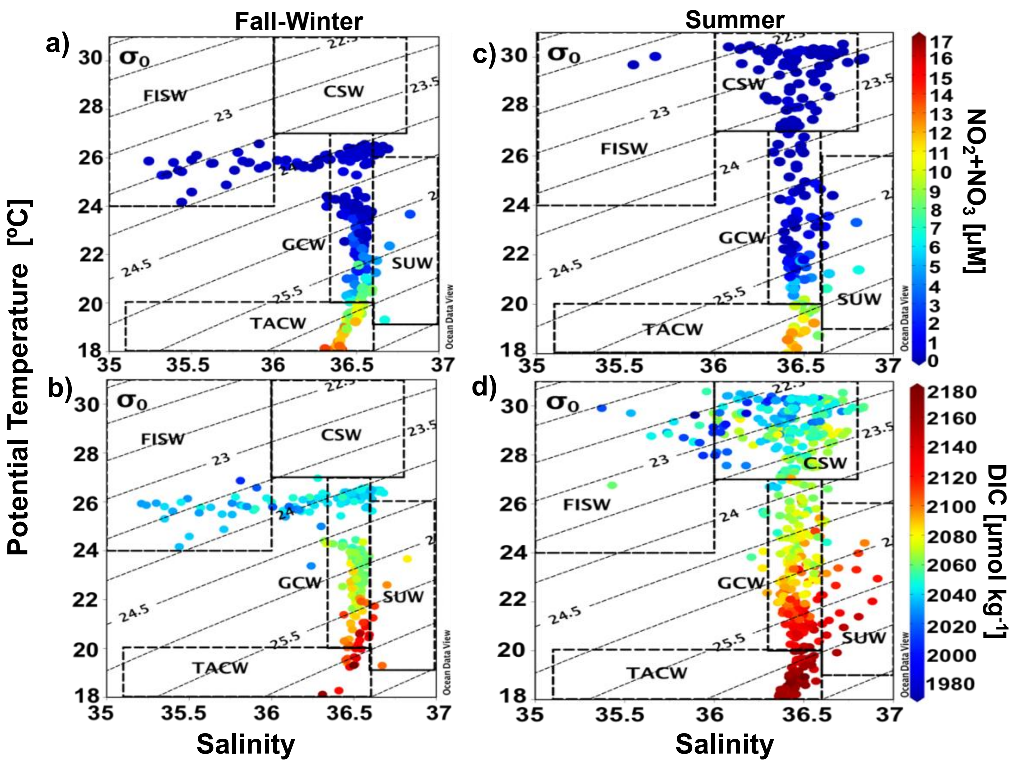

https://doi.org/10.5194/bg-2019-340
Preprint. Discussion started: 23 September 2019

Biogeosciences
Discussions

FIGURE 9:

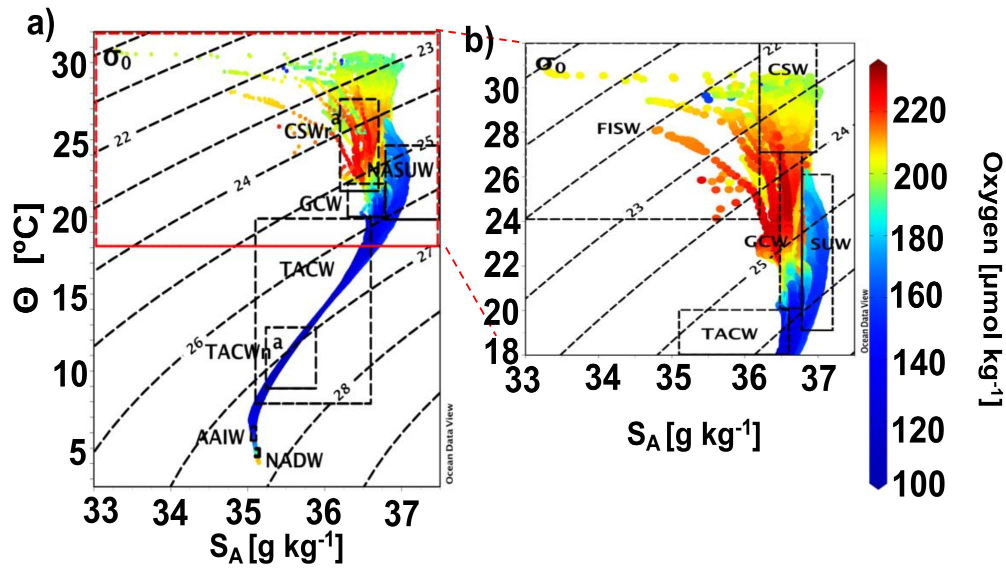

FIGURE 10:

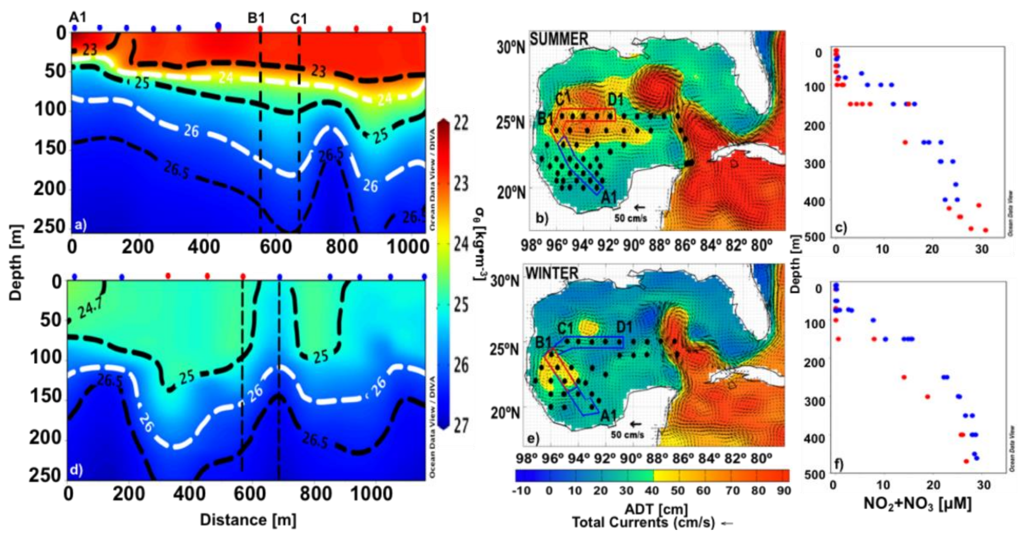

https://doi.org/10.5194/bg-2019-340
Preprint. Discussion started: 23 September 2019

Biogeosciences
Discussions
Open Access

FIGURE 11: